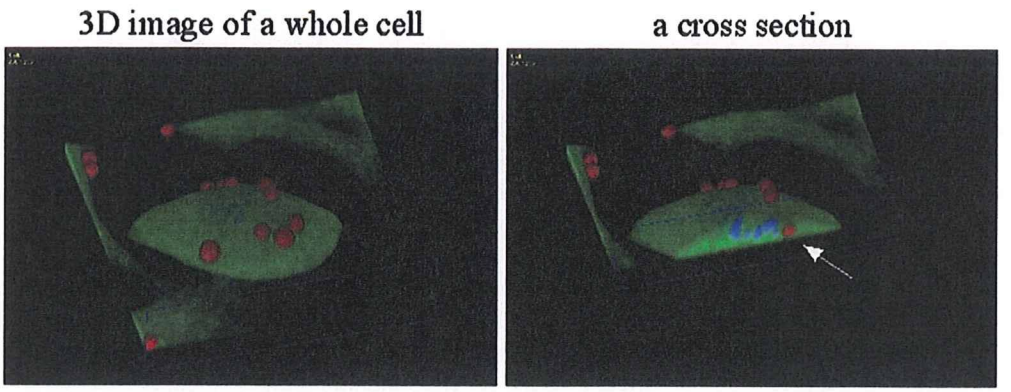

Fig. 7. Uptake of FluoSpheres (2.0 μm) by a CHL cell. Red indicates FluoSpheres. Green indicates cytoplasm stained with FITC. Blue indicates chromosomes stained with DAPI. The white arrow indicates an incorporated bead situated in the cross section.

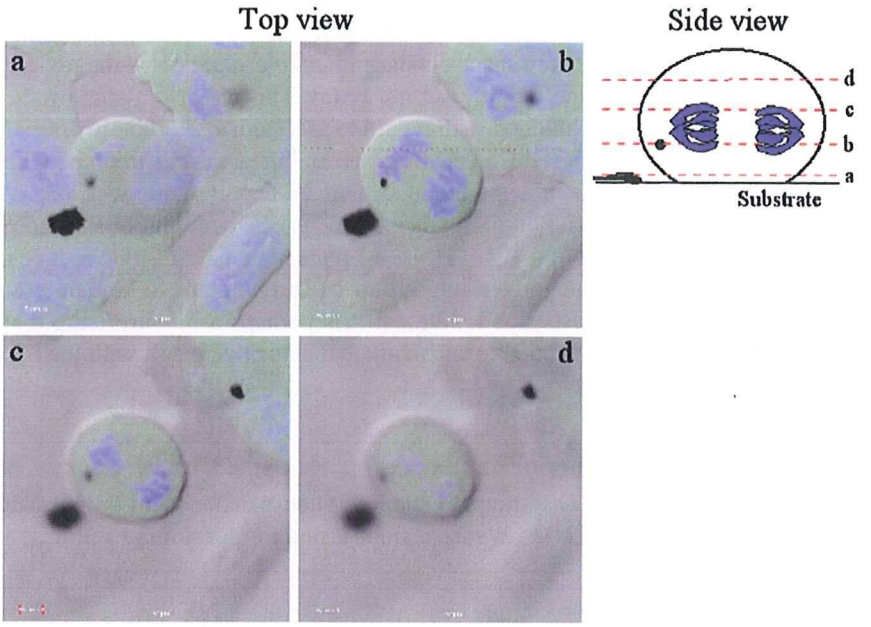

Fig. 8. Uptake of NHas by a CHL cell. NHas was observed on differential interference contrast microscopy (DIC). The photos show merged images of DIC and DAPI fluorescence. A mitotic cell (anaphase) with a particle inside is shown. Two bigger aggregates can be seen outside the round anaphase cell. Single slices are from (a) close to the bottom of the cell and just below the particle, (b) a plane above where the particle is in focus and (c,d) sections through the top of the cell.

4. Discussion

Among PS particles tested, the 4.45-μm particles showed the strongest cytotoxicity; smaller and larger particles showed less cytotoxicity. The results are similar to the report with quartz particles in the cultured monocytes [6]. The 0.1-μm particles did not show any cytotoxicity even at a high concentration of 1000 μg/ml. We tried to disperse NMs not only as homogenously but also as small as possible in the

suspension to be tested. We prepared six NHas suspensions with different particle size distribution by use of DMSO and ultrasonication. The cytotoxicity of these suspensions, however, was almost the same. The explanation is probably that the frequency of the 1.01–4.47 μm aggregates was similar and ranged from 40% to 60% in frequency. The reported findings here strongly suggest that sizes of aggregates need to be taken into consideration in evaluation of the biological safety of NMs.

Further, the physical characteristics of particles need to be taken into account. NHas was a hydrophobic black powder at hand. When suspended directly in water or the culture medium, NHas was adsorbed here and there on the wall of plastic tubes and pipettes. By using DMSO, the hydrophobic powder was almost perfectly collected in the culture medium, and more precise concentrations of material could be delivered to the cultures. The suspension remained homogenous for one month. This is good news not only for the *in vitro* but also the *in vivo* toxicology tests.

Miyawaki et al. reported the biological activity of NHas including the CA test with CHL cells [15]. The result of the CA test was the same as ours, i.e. negative. The concentrations tested for 48 h by Miyawaki et al. were different. They treated CHL cells up to 2.5 mg/ml. We could observe dividing cells (chromosomes) up to 200 μg/ml but not at higher concentrations. Miyawaki et al. did not show any data on particle size distribution in the 1% carboxymethyl cellulose sodium suspension used. The differences in dispersion methods may well explain the discrepancy and if so it underlines the need for physicochemical data on the aggregates in suspensions applied in evaluation of the toxicity of NMs.

In this study, PS particles induced polyploidy but not NHas. This effect is a sign of aberrant mitosis, and need further observations to be explained with regard to mechanism. Polyploidy is usually observed when chromosome distribution is aberrant or cleavage is inhibited during mitosis. Chrysotile B (an asbestos) induces polyploidy in the same experiment system; 39% polyploidy was observed at 5 μg/ml in the 48-h treatment (data not shown). Polyploidy is a characteristic endpoint of asbestos in the *in vitro* CA test [16]. When we concern about toxicity of NMs, we remember asbestos that induce mesothelioma and lung cancer in humans, and is categorized into group 1 (Carcinogenic to humans) by WHO/IARC [17]. PS particles are spherical and asbestos is fibrous. It is perhaps a bit surprising that PS particles induced polyploidy. Further tests are needed to substantiate the positive result with the PS particles.

5. Conclusion

We, here, propose the use of DMSO to prepare stable NM suspensions and the measurement of the mean size and the size distribution of NMs in suspensions tested for developing a precise *in vitro* safety evaluation system for NMs.

Acknowledgements

The Health and Labor Sciences Research Grants from the Ministry of Health, Labor, and Welfare of Japan financially supported this study (H19-IYAKU-IPPAN-015).

References

[1] L.E. Murr, K.M. Garza, K.F. Soto, A. Carrasco, T.G. Powell, D.A. Ramirez, P.A. Guerrero, D.A. Lopez and J. Venzor 3rd., Cytotoxicity assessment of some carbon nanotubes and related carbon nanoparticle aggregates and the implications for anthropogenic carbon nanotube aggregates in the environment, *Int. J. Environ. Res. Public Health* 2 (2005), 31–42.

[2] T. Xia, M. Kovochich, J. Brant, M. Hotze, J. Sempf, T. Oberley, C. Sioutas, J.I. Yeh, M.R. Wiesner and A.E. Nel, Comparison of the abilities of ambient and manufactured nanoparticles to induce cellular toxicity according to an oxidative stress paradigm, *Nano Lett.* 6 (2006), 1794–1807.
[3] B.B. Aam and F. Fonnum, Carbon black particles increase reactive oxygen species formation in rat alveolar macrophages *in vitro*, *Arch. Toxicol.* 81 (2007), 441–446.
[4] E. Herzog, A. Casey, F.M. Lyng, G. Chambers, H.J. Byrne and M. Davoren, A new approach to the toxicity testing of carbon-based nanomaterials: the clonogenic assay, *Toxicol. Lett.* 174 (2007), 49–60.
[5] J.J. Wang, B.J.S. Sanderson and H. Wang, Cyto- and genotoxicity of ultrafine TiO_2 particles in cultured human lymphoblastoid cells, *Mutat. Res.* 628 (2007), 99–106.
[6] K. Koshi, H. Hayashi, A. Hamada and H. Sakabe, The toxic effect of the various dusts on the intraperitoneal monocyte in rat, *Bull. Nat. Inst. Indust. Health* 6 (1961), 10–27.
[7] H. Yin, H.P. Too and G.M. Chow, The effects of particle size and surface coating on the cytotoxicity of nickel ferrite, *Biomaterials* 26 (2005), 5818–5826.
[8] K. Ajima, M. Yudasaka, T. Murakami, A. Maigné, K. Shiba and S. Iijima, Carbon nanohorns as anticancer drug carriers, *Mol. Pharm.* 2 (2005), 475–480.
[9] T. Murakami, J. Fan, M. Yudasaka, S. Iijima and K. Shiba, Solubilization of single-wall carbon nanohorns using a Peg–Doxorubicin conjugate, *Mol. Pharm.* 3 (2006), 407–414.
[10] M. Ishidate Jr. and S. Odashima, Chromosome tests with 134 compounds on Chinese hamster cells *in vitro* – a screening for chemical carcinogens, *Mutat. Res.* 48 (1977), 337–354.
[11] A. Matsuoka, M. Hayashi and M. Ishidate Jr., Chromosomal aberration tests on 29 chemicals combined with S9 mix *in vitro*, *Mutat. Res.* 66 (1979), 277–290.
[12] S. Iijima, M. Yudasaka, R. Yamada, S. Bandow, K. Suenaga, F. Kokai and K. Takahashi, Nano-aggregates of single-walled graphitic carbon nano-horns, *Chem. Phys. Lett.* 309 (1999), 165–170.
[13] A. Matsuoka, K. Isama and T. Tsuchiya, *In vitro* induction of polyploidy and chromatid exchanges by culture medium extracts of natural rubbers compounded with 2-mercaptobenzothiazole as a positive control candidate for genotoxicity tests, *J. Biomed. Mater. Res.* 75A (2005), 439–444.
[14] A. Matsuoka, T. Sofuni, N. Miyata and M. Ishidate Jr., Clastogenicity of 1-nitropyrene, fluorene, and mononitrofluorenes in cultured Chinese hamster cells, *Mutat. Res.* 259 (1991), 103–110.
[15] J. Miyawaki, M. Yudasaka, T. Azami, Y. Kubo and S. Iijima, Toxicity of single-walled carbon nanohorns, *ACS Nano* 2 (2008), 213–226.
[16] K. Koshi, N. Kohyama, T. Myojo and K. Fukuda, Cell toxicity, hemolytic action and clastogenic activity of asbestos and its substitutes, *Industrial Health* 29 (1991), 37–56.
[17] International Agency for Research on Cancer, *Asbestos*, IARC Monographs on the Evaluation of Carcinogenic Risk of Chemicals to Men, Vol. 14 (Suppl. 7), IARC, Lyon, France, 1987.

Effects of surface chemistry prepared by self-assembled monolayers on osteoblast behavior

Ryusuke Nakaoka,[1] Yoko Yamakoshi,[2] Kazuo Isama,[1] Toshie Tsuchiya[1]

[1]Division of Medical Devices, National Institute of Health Sciences, 1-18-1 Kamiyoga, Setagaya-ku, Tokyo 158-8501, Japan
[2]Departments of Radiology and Department of Chemistry,University of Pennsylvania, 231 S. 34th Street, Philadelphia, Pennsylvania 19104-6323

Received 27 August 2008; revised 8 October 2009; accepted 1 November 2009
Published online 00 Month 2009 in Wiley InterScience (www.interscience.wiley.com). DOI: 10.1002/jbma.a.32714

Abstract: A surface of biomaterials is known to affect the behavior of cells after their adhesion on the surface, indicating that surface characteristics of biomaterials play an important role in cell adhesion, proliferation, and differentiation. To assess the effects of functional groups on biomaterial surface, normal human osteoblasts (NHOsts) were cultured on surfaces coated with self-assembled monolayers (SAMs) containing various functional groups, and the adhesion, proliferation, differentiation, and gap junctional intercellular communication (GJIC) of the NHOsts were investigated. In the case of SAM with terminal methyl groups (hydrophobic surface), NHOst adhesion and proliferation was less prevalent. In contrast, NHOsts were adhered well on SAMs with hydroxyl, carboxyl, amino, phosphate, and sulfate group, which are relatively hydrophilic, their proliferation and differentiation level were dependent on the type of functional groups. Especially, when they were cultured on either SAMs with phosphate or sulfate group, both their alkaline phosphate activity and the calcium deposition by them were enhanced more than those cultured on a collagen-coated dish. More interestingly, GJIC of NHOsts, which has been reported to play a role in cell differentiation as well as homeostasis of cells, were not significantly different among the SAM surfaces tested. These suggest that a specific functional group on a material surface can regulate NHOst adhesion, proliferation, and differentiation via cell-functional group interaction without influencing their homeostasis. © 2009 Wiley Periodicals, Inc. J Biomed Mater Res Part A: 00A: 000–000, 2010

Key Words: self assembled monolayer, surface chemistry, cell differentiation, gap junctional intercellular communication

INTRODUCTION

Many cellular responses followed by an interaction with the biomaterials are mediated through signal transductions triggered by cellular recognition of their surface characteristics. Cells first recognize proteins adsorbed on the biomaterials, followed by various cellular responses. The extracellular matrix (ECM), consisting of numerous kinds of molecules such as proteins, polysaccharides, and proteoglycans, regulates the behavior of surrounding cells via the integrins to form tissues and organs precisely.[1,2] As the ECM provides an essential three-dimensional environment for cells to construct the tissues, many researches focused on the improvement of biocompatible materials by their modification, including artificial ECMs. It is known that first proteins, such as fibronectin and vitronectin, adsorb firstly onto the surface of materials, followed by cell adhesion onto the surface via recognition of the proteins. The modification of biomaterial surfaces with various peptides or proteins composing the ECM can result in the improvement of the adhesion, proliferation, and differentiation of the cells.[3–8] It has been reported that conformation and adhesion behavior of proteins are influenced by the surface characteristics of the materials, and functions of cells adhering on the surface are regulated via the structure of the adsorbed proteins,[9] indicating that surface characteristics of the materials are important factors in controlling cell behavior in desired manner via adsorbed proteins. Thus, a systematic control of surface characteristics may be one way to regulate cell behavior interacted with the surface, in other words, it can regulate the biocompatibility of biomaterials.

During this decade, many studies on self-assembled monolayers (SAMs) of alkanethiolates on gold to control interfacial characteristics have been reported.[10–14] Long-chain alkanethiolates can adsorb onto a gold surface in the solution forming well-packed and highly oriented monolayers by the specific reaction of thiol to gold and van der Waals interaction of long alkyl chain. By using alkanethiolate derivatives with terminal functional groups, a surface modified with a specified functional group can be prepared easily to study an interaction between the simplified model material surface covered with the specified functional group and cells. Many studies of cell behavior on SAM surfaces with systematic patterns from hydrophobic and hydrophilic groups have been reported, but studies on an effect of specific functional groups such as amino (positively charged group), phosphate (possible site to initiate hydroxyapatite

Correspondence to: R. Nakaoka; e-mail: nakaoka@nihs.go.jp
Contract grant sponsors: Health and Labour Sciences Research Grants for Research on Advanced Medical Technology; Research on Regenerative medicine and Research on Regulatory Science of Pharmaceuticals, Medical Devices by Ministry of Health, Labour and Welfare

nucleation), and sulfate groups are not easily found although these groups can be expected to affect cell behavior via interaction with endogenous growth factors. We have been working on this and have reported that polysaccharides modified with sulfated groups enhance differentiation level of interacted cells *in vitro*,[15] suggesting a preferable property of sulfated groups on biocompatibility of materials. Therefore, studies on an interaction between a specified functional group such as a sulfated group and cells will satisfy one of our interests in mechanisms of sulfated groups on cell fate, and give valuable information of key factors regulating biocompatibility of various biomaterials.

In this study, various SAM surfaces covered with a specific functional group, such as alkyl, carboxyl, hydroxyl, amino, phosphorylated, or sulfated group, were prepared. After culturing normal human osteoblasts (NHOsts) on each surface, their proliferation and differentiation levels were measured to evaluate influences of surface functional groups on cell behavior. Also gap junctional intercellular communication (GJIC) level of the NHOsts on various SAM surfaces was measured, as this has been reported to play a very important role in the maintenance of cell homeostasis,[16] and we have been interested in the effects of model biomaterials on the GJIC level of the cells as an index of biocompatibility of biomaterials.[17–22] In this study, basic findings of interaction between cells and surface functional groups are described, which will be important for designing more biocompatible and functional biomaterials in the near future.

MATERIALS AND METHODS

Chemicals

Chemicals for the preparation of SAM surfaces such as 11-hydroxy-1-undecanethiol, 10-carboxy-1-decanethiol, and 11-amino-1-undecanethiol, were purchased from Dojindo laboratories (Kumamoto, Japan). The 1-dodecanthiol and other chemicals used for the preparation of SAM-OSO_3H and SAM-OPO_3H_2 were purchased from Wako Pure Chemicals, Inc. (Osaka, Japan) unless stated.

Preparation of gold-coated coverslips

Gold-coated coverslips for the experiments were prepared by ion spattering coating of gold with 15 nm in thickness onto glass coverslips (Matsunami Glass Ind., Ltd. Osaka, Japan) using JFC-1500 (JEOL Ltd., Tokyo, Japan). For the preparation of SAM with terminal methyl groups (SAM-CH_3), coverslips were precoated with chromium (1 nm in thickness) by electron-beam evaporation to avoid detaching the gold coating due to the hydrophobicity of the SAM surface.

Preparation of self-assembled monolayer (SAM)-covered coverslips (SAM-CH_3, SAM-OH, SAM-COOH and SAM-NH_2)

A SAM surface covered with terminal methyl (SAM-CH_3), hydroxyl (SAM-OH), carboxyl (SAM-COOH), or amino group (SAM-NH_2) on a coverslip was prepared by simply immersing a gold-coated coverslip into ethanol solution (1 m*M*) of corresponding commercially available alkanethiol derivatives for 24 h at room temperature. The obtained SAM-covered coverslips were washed by ethanol for several times, followed by drying *in vacuo*. The obtained SAMs are schematically described in Figure 1. F1

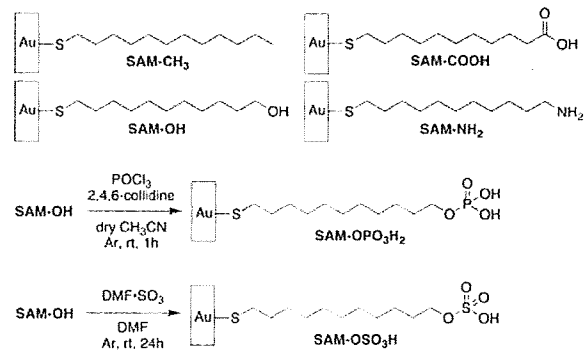

FIGURE 1. A schematic description of SAM surfaces prepared in this study.

Preparation of SAM-OPO_3H_2-covered coverslip

A phosphorylated SAM surface (SAM-OPO_3H_2) was prepared using the method described by Tanahashi and Matsuda.[23] Briefly, the gold-coated coverslip covered with SAM-OH was phosphorylated by the addition of 0.2*M* phosphorus oxychloride and 0.2*M* 2,4,6-collidine in dry CH_3CN under Ar atmosphere. The reaction was carried out for 1 h at room temperature under Ar atmosphere. The resulted coverslip with SAM-OPO_3H_2 was then washed with CH_3CN thoroughly, and water for several times, then dried *in vacuo* at room temperature. Scheme of this reaction is shown in Figure 1.

Preparation of SAM-OSO_3H-covered coverslip

A sulfated SAM surface (SAM-OSO_3H) was prepared by sulfation of hydroxyl groups using sulfertrioxide dimethylformamide complex (DMF-SO_3), which was originally reported as a sulfation method of hydroxyl groups of polysaccharides.[21,24] Briefly, the coverslip of SAM-OH was immersed in dry *N,N'*-dimethylformamide (DMF), followed by the addition of DMF-SO_3 (Sigma-Aldrich, St. Louis, MO) under Ar atmosphere. The reaction was carried out for 24 h at room temperature under Ar atmosphere. The obtained coverslip with SAM-OSO_3H was washed for several times with DMF and water, and then dried *in vacuo* at room temperature. A scheme of this reaction is shown in Figure 1 as well.

Surface characterization of SAM-covered coverslips

Water contact angles of all prepared SAM-covered coverslips were measured with the sessile drop method. More than five measurements were carried out for each SAM-covered coverslip. Surface chemical compositions of the SAM-covered coverslips were analyzed by electron spectroscopy for chemical analysis (ESCA-3200, Shimadzu Co., Kyoto, JAPAN).

Cell culture

Normal human osteoblasts (NHOst) were purchased from Cambrex Bioscience Walkersville Inc. (Walkersville, MD). The standard culture of NHOst was performed using alpha minimum essential medium (Gibco, Grand Island, NY) containing 20% fetal calf serum (FCS) (Kokusai Shiyaku Co., Ltd., Tokyo Japan). The cells were maintained in incubators under standard conditions (37°C, 5 %-CO_2-95 %-air, saturated humidity). All assays were performed using alpha minimum essential medium containing 20% FCS, supplemented with 10 m*M* beta-glycerophosphate. The various SAM-covered coverslips were placed in the wells of 12-well plates and NHOsts (4×10^4 cells/well/1 mL medium) were inoculated on them. In each experiment, the medium was changed for three times and their differentiation level was evaluated after a 1-week incubation.

Proliferation and differentiation of NHOsts cultured on various SAM-covered coverslips

The proliferation of NHOst cells cultured on SAM-covered coverslips was estimated by Tetracolor One assay reagent (Seikagaku Co., Tokyo, Japan), which incorporates an oxidation–reduction indicator for detecting cellular metabolic activity. After a 1-week incubation of NHOsts, 50 μL of Tetracolor One solution was added to each test dish filled with 1 mL of a culture medium, followed by a further 2 h incubation. The absorbance of the supernatant at 450 nm was measured by μQuant spectrophotometer (Bio-tek Instruments, Inc., Winooski, VT).

Estimation of alkaline phosphatase (ALP) activity was performed according to an original procedure by Ohyama et al.[25] After estimating the proliferation of the NHOst cells cultured on the SAM-covered coverslips, the cells were washed by phosphate-buffered saline (PBS(−)), followed by the addition of 1 mL of 0.1*M* glycine buffer (pH 10.5) containing 10 m*M* $MgCl_2$, 0.1 m*M* $ZnCl_2$, and 8 m*Mp*-nitrophenylphosphate sodium salt. After incubating the cells at room temperature for 7 min, the absorbance of the solution at 405 nm was detected using μQuant to evaluate the ALP activity of the tested cells.

The amounts of calcium deposited by the cell during a 1-week incubation were measured as follows. After fixing the cells in PBS(−) containing 3% formaldehyde, the cells were washed with PBS(−), and then 0.5 mL of 0.1*M* HCl was added to each well. The amounts of calcium dissolved in HCl were estimated using a calcium detecting kit (Calcium-C test Wako, Wako, Osaka, Japan) according to manufacturer's instruction.

Measurements of GJIC activity

NHOst cultured on SAM-covered coverslips were subjected to fluorescence recovery after photobleaching (FRAP) analysis to evaluate the effect of these surfaces on the GJIC. FRAP analysis was carried out according to the procedure of Wade et al.[26] with some modifications.[20] Briefly, NHOst were plated and incubated for 1 day on the SAM-covered coverslips. After incubated with a fluorescent dye, 5,6-carboxyfluorescein diacetate in PBS(+), the cells contacting at least two other cells were subjected to FRAP analysis under Ultima-Z confocal microscope (Meridian Instruments, Okemos, MI). The cells were photobleached with a 488 nm beam, and recovery of fluorescence intensity was subsequently monitored for 4 min. The data obtained from more than seven independent cells were expressed as the average ratio of the fluorescence recovery rate to the rate obtained from NHOst cultured on a collagen-coated dish as standard experiments.

Connexin 43 mRNA expression in NHOsts

To estimate effects of the surface functional group on mRNA expression of connexin43 protein, which plays an important role in GJIC by forming channels between neighboring cells, a real time PCR technique was applied. Briefly, total RNA from NHOsts cultured on various functional groups was isolated by RNeasy microprep kit (QIAGEN, Valencia, CA) per the manufacturer's instruction. After its reverse transcription, a real time PCR was performed utilizing the primers for connexin43, LightCycler FastStart DNA master SYBR green I kit (Roch Applied Science, Penzberg, Germany) and LightCycler 4 (Roche Applied Science). To normalize the data, mRNA expression of a housekeeping gene, glyceraldehyde 3-phosphate dehydrogenase (GAPDH), was also determined using LightCycler primer set for GAPDH (Roche Applied Science). Primer sequences for connexin43 are shown below:

Forward: 5′-GGGCTAATTACAGTGCAG-3′
Reverse: 5′-CATGTCCAGCAGCTAGTT-3′

Statistic analysis

All data were expressed as mean values ± standard deviation of the obtained data. The Fisher-Tukey criterion, calculated by inerSTAT-a v1.3 (freeware, published by Instituto Nacional de Enfermedades Respiratorias), was used to control for multiple comparisons and to compute the least significant difference between means.

RESULTS

Table I shows contact angle against water and elemental signal ratios of prepared coverslips covered with various SAMs. The signal ratio against a carbon signal detected in the same surface by ESCA was calculated from the signal area and the sensitivity factor of each element. If a signal area recorded on ESCA was lower than 10^3 or the calculated value was lower than 1×10^{-3}, the results were not described in the table. As shown in Table I, contact angle measurements revealed that while SAM-CH_3 had a hydrophobic surface, others SAMs except for SAM-NH_2 had hydrophilic ones compared with the intact gold-coated surface. The contact angle of SAM-OH was significantly lower than any other SAM surfaces. After a reaction from SAM-OH to SAM-OPO_3H_2, the contact angle was significantly increased, suggesting that the reaction proceeded successfully. Also as shown in Table I, the ratios of atomic concentration of nitrogen, phosphorus, and sulfur (N/C, P/C, and S/C) calculated from raw signal areas were detected only from SAM-NH_2, SAM-OPO_3H_2, and SAM-OSO_3H, respectively, indicating that

T1

TABLE I. Surface Characterization of SAMs by Contact Angle and Elemental Signal Ratios Against Carbon

		SAMs Modifying Surfaces					
	Gold (Control)	SAM-OH	SAM-OSO_3H	SAM-COOH	SAM-OPO_3H_2	SAM- NH_2	SAM-CH_3
Contact Angle	64.4 ± 2.1	40.1 ± 14.2*,†	44.3 ± 10.2	51.7 ± 14.5	59.0 ± 13.7*	65.0 ± 9.8	102.9 ± 3.0†
Elemental signal ratios							
O/C	3.2×10^{-3}	2.9×10^{-3}	6.8×10^{-3}	4.6×10^{-3}	4.8×10^{-3}	2.2×10^{-3}	–
N/C	–	–	–	–	–	1.8×10^{-3}	–
P/C	–	–	–	–	2.1×10^{-3}	–	–
S/C	–	–	2.2×10^{-3}	–	–	–	–

* $p < 0.05$ between SAM-OH and SAM-OPO_3H_2.
† $p < 0.01$ against Au.

all desired SAM surfaces with specific functional groups were successfully prepared.

F3 F2 Figures 2 and 3 show light micrographs of NHOsts cultured on each SAM surface for 1 day and 1 week. When NHOsts were cultured on a gold-coated coverslip for 1 day, the number of NHOsts observed was apparently lower [Fig. 2(B)] than that on a collagen-coated culture plate [Fig. 2(A)]. After 1-week incubation, the surface of gold-coated coverslip was fully covered with NHOsts, indicating that the NHOsts could proliferate on the intact gold surface [Fig. 3(B)]. The numbers of NHOsts adhered on the gold surface with various SAMs were influenced by the functional groups covering the SAMs as follows. Less NHOsts could adhere on a SAM-CH_3, the most hydrophobic surface among the SAM surfaces used in this study, than those on the gold surface [Figs. 2(C) and 3(C)]. The NHOsts on the SAM-CH_3 were tended to aggregate after 1-day culture [Fig. 2(C)] and likely to detach from the surface during 1-week culture as no aggregates and few stretched NHOsts were observed after 1 week [Fig. 3(C)]. On the other hand, NHOsts adhered on other SAM surfaces such as SAM-COOH, SAM-OH, SAM-OPO_3H_2 and SAM-OSO_3H could be observed more than on the gold surface, as shown in Figure 1(D,E,G,H). Judging from the number of nodules observed in Figure 3, it is likely that there is no effect of functional groups in between the hydrophilic SAM surfaces on differentiation level of NHOsts.

T2 Table II summarizes the relative amount of cell number, ALP activity, and the deposited calcium of NHOsts after 1-week culture on various SAMs. Although differentiation levels of NHOsts on hydrophilic functional groups of SAM were not significantly different by the observation of the nodule number (Fig. 3), the functional groups apparently influenced both ALP activity of the NHOsts and the amount of deposited calcium as well as the cell number ratio adhering on the surface as shown in Table II. When NHOsts were cultured on SAM-CH_3 surface, not only the cell number but also their ALP activity were low and the amount of deposited calcium per cell were under detection limit. On the contrary, when NHOsts were cultured on SAM-OH, SAM-COOH, or SAM-NH_2, the cell number, the ALP activity and the deposited calcium amounts per cell were not significantly different from those observed on a gold surface. Interestingly, when NHOsts were cultured on SAM-OPO_3H_2 or SAM-OSO_3H, their ALP activity and the amounts of calcium deposition per cell increased although the cell number ratio was about one-third to half of that observed on a gold surface.

To estimate the effects of functional groups on another cell function, GJIC level of NHOsts on various SAM surfaces were measured after 1-day incubation (Table III). In addition, expression levels of connexin43 mRNA in NHOsts on the various functional groups were measured by real-time PCR (Fig. 4). Although it was observed that their differentiation level was influenced by the functional group on SAM surfaces, statistical differences in neither the GJIC level nor the expression level of connexin43 mRNA during 1-week culture were observed among the SAM surfaces tested in comparison with that of NHOsts on a collagen-coated dish at the same time period of their culture.

T3 F4

DISCUSSION

Several studies have been reported that surface chemical properties are responsible for behavior of attached cells, for example, their adhesion, proliferation, and differentiation on the surface as well as surface topography such as microfabricated grooves and pits.[9–12,27,28] Usually, a cell adheres not directly on a surface of a material but on preadsorbed proteins on the material, originally contained in the culture medium. Interaction of the preadsorbed proteins with a material surface is important in cell attachment and protein adsorption is influenced by surface properties, such as chemical composition, surface charge, and a hydrophilicity/hydrophobicity balance of surface.[9] Therefore, SAM is an ideal surface to investigate effects of the chemical and physico-chemical property on cell behavior as the surface covered by single chemical group can be prepared easily.

Changes in contact angles and elemental signal ratio against carbon signals of the prepared SAM surfaces (Table I) indicated that SAM surfaces covered with various chemical groups could be prepared successfully by the methods described in "Materials and Methods" section. Although chlorosulfonic acid is a common reagent to convert hydroxyl groups of SAM-OH to sulfate group,[29] we used DMF-SO_3 for the preparation of SAM-OSO_3H in this study. In the trial of substitution reaction by chlorosulfonic acid, it was found to be difficult to remove all by-products adsorbed on the coverslip without detaching a gold coating, thus modest

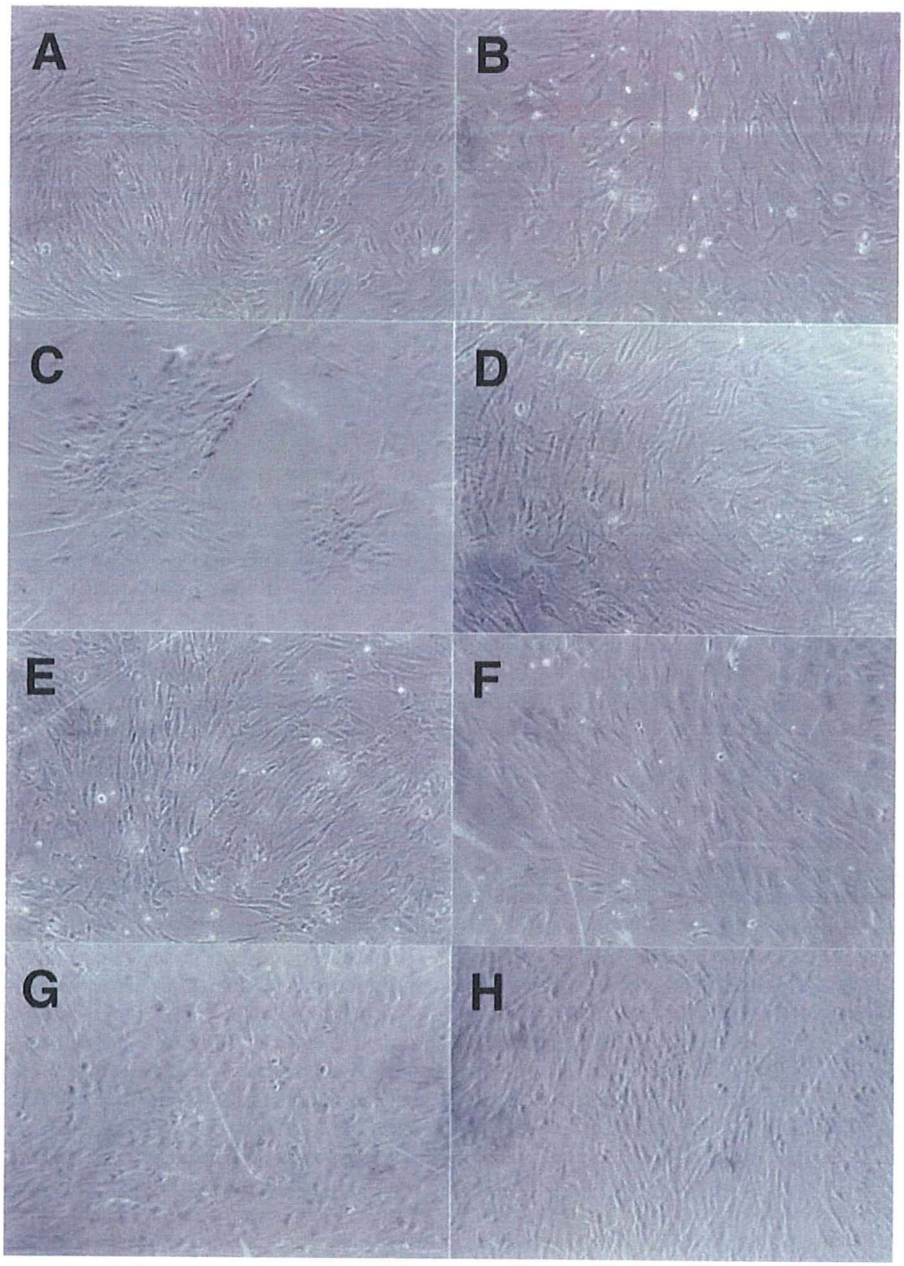

FIGURE 2. Light micrograph of NHOsts cultured on various SAM surfaces for 1 day. (Original magnification is ×40.) NHOsts were cultured on a collagen-coated dish (A), gold-coated coverslip (B), SAM-CH_3 (C), SAM-COOH (D), SAM-OH (E), SAM-NH_2 (F), SAM-OPO_3H_2 (G), and SAM-OSO_3H (H). [Color figure can be viewed in the online issue, which is available at www.interscience.wiley.com.]

condition reaction, which is often applied for sulfation reaction of hydroxyl groups in polysaccharides with fewer by-products, was employed. In fact, an apparent S/C signal was detected as shown in Table I, indicating the sulfate group was successfully introduced to the surfaces by the employed reaction in good yield.

Effect of chemical groups on cell attachment has been studied as well as protein adsorption utilizing SAM. It has been reported that the number of cell adhering on various surfaces is influenced by the physico–chemical properties of the surfaces such as hydrophilic/hydrophobic balance, which is closely related to contact angles.[11,12,27,30–33] In this study, modification of the gold surface with SAM changed the number of NHOsts adhering on the surface depending on the functional groups of the SAM (Fig. 2). Less NHOsts could adhere on a SAM-CH_3, the most hydrophobic surface among the prepared SAM surfaces, than those on the gold surface. The NHOsts observed on it were tend to aggregate

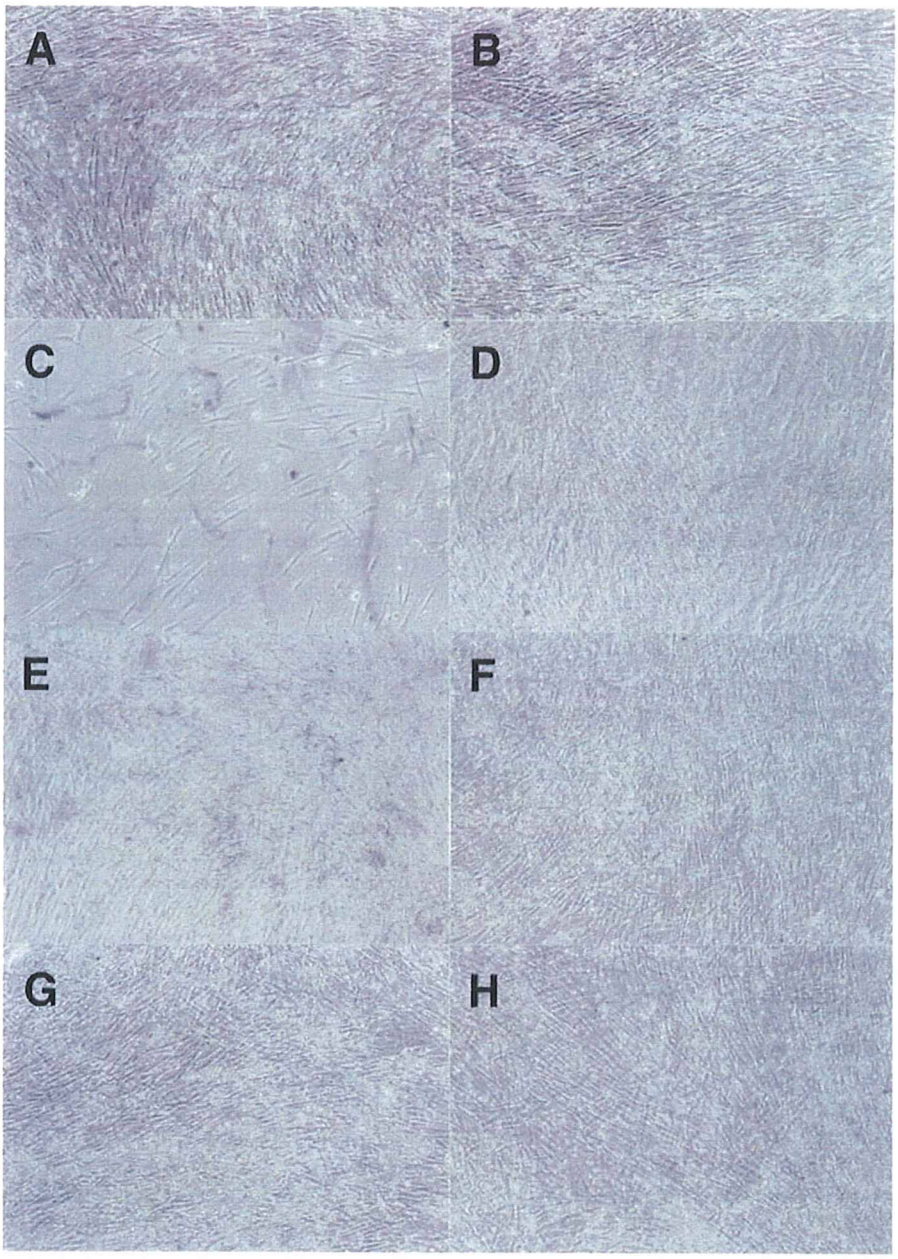

FIGURE 3. Light micrograph of NHOsts cultured on various SAM surfaces for 7 days. (Original magnification is ×40.) NHOsts were cultured on a collagen-coated dish (A), gold-coated coverslip (B), SAM-CH_3 (C), SAM-COOH (D), SAM-OH (E), SAM-NH_2 (F), SAM-OPO_3H_2 (G), and SAM-OSO_3H (H). [Color figure can be viewed in the online issue, which is available at www.interscience.wiley.com.]

and likely to detach from it during 1-week culture as no aggregates and a few stretched NHOsts were observed on it as shown in Figure 3. On the other hand, NHOsts could adhere on other SAM surfaces more than on the gold surface, indicating that the surfaces covered with functional groups such as amino, carboxyl, hydroxyl, phosphate, and sulfate groups have a suitable hydrophilic/hydrophobic balance not to interfere cell adhesion them. As adhesion and spreading behaviors of osteoblasts on materials have been reported to depend on vitronectin and fibronectin primarily adsorbed on the surfaces,[34,35] it may be indispensable to investigate an interaction between various functional groups and these two proteins influencing there adsorption behavior and possible conformation changes to clarify the mechanism of cell adhesion on the interacted-functional groups more precisely.

The ALP activity and deposited calcium amount were measured for estimating differentiation level of NHOsts

ID: thambikkanue | Black Lining: [ON] | Time: 13:52 | Path: N:/3b2/JBMM/Vol00000/090343/APPFile/C2JBMM090343

TABLE II. The Cell Number, Alkaline Phosphatase Activities, and Deposited Calcium Amounts of NHOsts Cultured on Several Kinds of Prepared SAM Surfaces after 1-week Incubation

Samples	The Cell Number Ratio (%)	$\frac{\text{ALP Activity}}{\text{The Cell Number}}$ (%)	$\frac{\text{Calcium Amounts}}{\text{The Cell Number}}$ (μg/ratio)
Gold	100.0 ± 4.9	100.0 ± 10.0	8.1 ± 1.6
SAM-OH	107.8 ± 2.2	119.7 ± 6.4	8.7 ± 2.3
SAM-OSO_3H	50.8 ± 15.4*	150.1 ± 55.0	33.4 ± 13.5
SAM-COOH	93.2 ± 33.9	100.2 ± 6.8	11.6 ± 2.5
SAM-OPO_3H_2	37.5 ± 4.2*	147.5 ± 9.4	57.0 ± 25.2**
SAM-NH_2	106.1 ± 8.6	112.1 ± 4.3	8.5 ± 1.1
SAM-CH_3	17.1 ± 10.3*	34.8 ± 26.0*	Not detected
Collagen-dish	156.7 ± 3.1†	119.3 ± 6.0	15.5 ± 2.9

The cell number and the alkaline phosphatase activities were expressed as a ratio of against those on gold-coated coverslip. Both the alkaline phosphatase activities and the calcium amounts were normalized by the cell number.

* $p < 0.05$ against "Gold"and SAM-COOH group, and $p < 0.01$ against other SAM.

** $p < 0.05$ against "Gold."

† $p < 0.01$ against all other groups.

cultured on prepared SAM surfaces (Table II). When NHOsts were cultured on SAM-CH_3 surface, not only the cell number but also their ALP activity decreased and the amounts of deposited calcium per cell were not detected. This suggests that NHOsts cannot maintain their differentiation level when they cannot adhere on the surface. When NHOsts were cultured on SAM-OH, SAM-COOH, or SAM-NH_2, their number, ALP activity and deposited calcium amounts per cell were almost the same as those observed on a gold surface. These indicate that a surface property that affects cell adhesion level is a one of factors to regulate differentiation level of NHOst. Interestingly, when NHOsts were cultured on SAM-OPO_3H_2 or SAM-OSO_3H, ALP activity of NHOsts and the amounts of calcium deposition per cell increased although the cell number ratio was about a one-third to a half of that observed on a gold surface. Tanahashi and Matsuda have reported that a surface covered with negatively charged chemical groups enhances the growth rate of apatite when it was soaked in a simulated body fluid because of interaction between calcium ion and the surface.[23] Interestingly, an apatite growth rate on SAM-OPO_3H_2 has been reported to be higher than that on SAM-COOH,[23] suggesting an equilibrium constant of the functional groups, which determines their negative charge level in physiological pH, affects strength of the interaction. In this study, SAM-COOH cultured with NHOsts showed almost the same calcium deposition as SAM-OH and gold surface, while SAM-OPO_3H_2 and SAM-OSO_3H showed calcium deposition 4 to 7 times as much as other surfaces tested. In addition, ALP activity of NHOsts on these two SAM surfaces was higher than any other surfaces including collagen-coated dish, which is normally utilized for a culture of NHOsts. Table I indicates that contact angle of SAM-OH is almost similar to that of SAM-OSO_3H and there are no statistical differences among contact angles of 3 SAMs, SAM-OSO_3H, SAM-COOH, and SAM-OPO_3H_2. Therefore, these findings suggest that chemical composition of the surfaces, which determines its ionic charge and zeta potentials of surfaces in physiological pH, may be one of key factors to regulate differentiation level of osteoblasts more than their hydrophilic/hydrophobic balance. As different ionic charge of SAM surfaces has been reported to influence protein adsorption as well as their hydrophilic/hydrophobic balances,[36] it is necessary to evaluate actual zeta potentials of prepared SAM surfaces in physiological pH before investigating the interaction between various functional groups and proteins including vitronectin and fibronectin, which may provide valuable information of effects of the functional groups on the cell differentiation level as well.

Although the differentiation level of NHOsts was influenced by the functional groups on SAM surfaces, their GJIC level after 1-day culture were almost the same as that of NHOsts cultured on a collagen-coated dish as a control experiment, irrespective of the type of functional group (Table III). This indicates that NHOsts interacting with these functional groups can maintain their homeostasis, irrespective of the kind of the functional group. Although GJIC has been reported to play a role in differentiation of osteoblasts,[37,38] the effect of the functional group on differentiation level of NHOsts observed in this study may be

TABLE III. Gap Junctional Intercellular Communication Activity of NHOst on Various SAM Surfaces after 1-day Incubation Measured by FRAP Analysis Technique

	Collagen-Coated Dish (control)	Gold	SAMs Modifying Surfaces					
			SAM-OH	SAM-OSO_3H	SAM-COOH	SAM-OPO_3H_2	SAM-NH_2	SAM-CH_3
GJIC activity (Ratio vs. control)	1.00 ± 0.38	1.00 ± 0.69	1.11 ± 0.46	0.92 ± 0.47	0.87 ± 0.41	1.12 ± 0.41	1.15 ± 0.46	1.24 ± 0.54

All values were calculated as a ratio of the activity against that obtained from NHOsts on a collagen-coated culture dish (control). (n = 12–14).

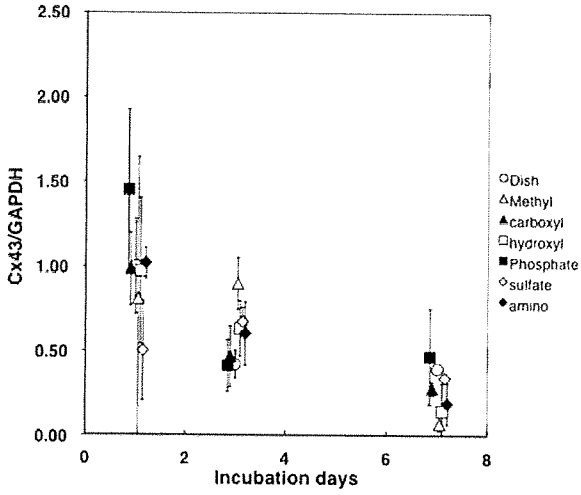

FIGURE 4. Expression levels of connexin43 mRNA in NHOsts cultured on various SAM surfaces ($n = 3$). The expression levels of the connexin43 mRNA were normalized by GAPDH mRNA expression level estimated from the same samples of total RNA and expressed as a ratio against the expression level in NHOsts on a collagen-coated culture dish after 1-day culture. NHOsts were cultured on a collagen-coated dish (open circle), SAM-CH_3 (open triangle), SAM-COOH (closed triangle), SAM-OH (open square), SAM-OPO_3H_2 (closed square), SAM-OSO_3H (open diamond), and SAM-NH_2 (closed diamond).

independent of their GJIC function. It was also expected that GJIC of NHOsts on SAM-CH_3 would be different from others since less NHOst proliferation on the SAM suggested a possible perturbation in homeostasis of the NHOsts. Decrease in the cell number on the SAM after 1-week incubation, however, made GJIC measurement unable because few cells contacting with two other neighboring cells were found. On the other hand, the GJIC after 1-week culture did not show any statistical differences between NHOsts on other tested SAM surfaces and those on a collagen-coated culture dish (data not shown). In addition, Figure 4 has revealed that surface functional groups of SAM do not affect mRNA expression level of connexin43 during 1-week culture, indicating that the functional group do not affect signal cascades of connexin43 expression in NHOsts. To study effects of the functional group as well as hydrophilic/hydrophobic balance of the surface on GJIC more in detail, changes in GJIC level of cells on the surfaces are under investigation utilizing metabolic cooperation assay system. Results of the study will be reported in near future. However, this study suggests that an enhancement of differentiation level of NHOsts induced by phosphorylated or sulfate group on the surface is triggered by a direct interaction between the chemical group and NHOsts, followed by signal cascades in which GJIC does not participate. In fact, sulfated polysaccharides have been reported to affect expression of several genes relating to cell differentiation,[15] but a mechanism of the sulfated group to affect the expression of these genes remains to be clarified. The details of the interaction and the signal cascades will be clarified in future studies.

CONCLUSIONS

This study suggests that the functional groups covering surface have the potential to control attachment, proliferation, and differentiation of NHOsts cultured on it. Figures of NHOsts after 1-day culture and the cell numbers estimated after 1-week culture indicate that hydrophilic/Hydrophobic balance of the surfaces may be one of key factors to regulate attachment and proliferation of NHOsts on the surfaces. Although the proliferation level decreased, the surface covered with either phosphate or sulfate group showed an enhancement in differentiation level of cultured NHOsts through unidentified signal cascades triggered by these functional groups and independent of GJIC. This suggests that ionic charge level of the functional groups is one of key factors to regulate osteogenic differentiation on the surfaces more than hydrophilic/hydrophobic balance of the surfaces. Further studies are necessary for clarifying the mechanisms of different differentiation levels of NHOsts induced by interaction with the functional groups as well as for future applications of SAMs in the fields of medical devices and tissue engineering.

ACKNOWLEDGMENTS

Authors are grateful to Professor Toshiaki Enoki and Associate Professor Kenichi Fukui, Tokyo Institute Technology for their kind permission to utilize electron-beam evaporation equipment for chromium precoating. Authors are also grateful to Dr. Rumi Sawada, Division of Medical Devices, NIHS, Japan, for her kind support in real-time PCR experiments.

REFERENCES

1. Adams JC, Watt FM. Regulation of development and differentiation by the extracellular matrix. Development 1993;117:1183–1198.
2. Peterson WJ, Tachiki KH, Yamaguchi DT. Extracellular matrix alters the relationship between thymidine incorporation and proliferation of MC3T3-E1 cells during osteogenesis *in vitro*. Cell Prolif 2002;35:9–22.
3. Hirano Y, Okuno M, Hayashi T, Goto K Nakajima A. Cell-attachment activities of surface immobilized oligopeptides RGD, RGDS, RGDV, RGDT, and YIGSR toward five cell lines. J Biomater Sci Polym Ed 1993;4:235–243.
4. Alsberg E, Anderson KW, Albeiruti A, Rowley JA, Mooney DJ. Engineering growing tissues. Proc Natl Acad Sci 2002;99: 12025–12030.
5. Bisson I, Kosinski M, Ruault S, Gupta B, Hilborn J, Wurm F, Frey P. Acrylic acid grafting and collagen immobilization on poly(ethylene terephthalate) surfaces for adherence and growth of human bladder smooth muscle cells. Biomaterials 2002;23:3149–3158.
6. Nakaoka R, Tsuchiya T. Neural differentiation of midbrain cells on various protein-immobilized polyethylene films. J Biomed Mater Res 2003;64:439–446.
7. Masters KS, Shah DN, Walker G, Leinwand LA, Anseth KS. Designing scaffolds for valvular interstitial cells: Cell adhesion and function on naturally derived materials. J Biomed Mater Res A 2004;71:172–180.
8. Kong HJ, Boontheekul T, Mooney DJ. Quantifying the relation between adhesion ligand-receptor bond formation and cell phenotype. Proc Natl Acad Sci 2006;103:18534–18539.
9. Wilson CJ, Clegg RE, Leavesley DI, Pearcy MJ. Mediation of biomaterials-cell interactions by adsorbed proteins: A review. Tissue Eng 2005;11:1–18.
10. Ulman A. Formation and structure of self-assembled monolayers. Chem Rev 1996;96: 1533–1554.

11. Mrksich M, Whitesides GM. Using self-assembled monolayers to understand the interactions of man-made surfaces with proteins and cells. Annu Rev Biophys Biomol Struct 1996;25:55–78.
12. Senaratne W, Andruzzi L, Ober CK. Self-assembled monolayers and polymer brushes in biotechnology: Current applications and future perspectives. Biomacromol 2005;6:2427–2448.
13. Fujimoto H, Yoshizako S, Kato K, Iwata H. Fabrication of cell-based arrays using micropatterned alkanethiol monolayers for the parallel silencing of specific genes by small interfering RNA. Bioconjugate Chem 2006;17:1404–1410.
14. Shin SK, Yoon HJ, Jung YJ, Park JW. Nanoscale controlled self-assembled monolayers and quantum dots. Curr Opin Chem Biol 2006;10:423–429.
15. Nagira T, Nagahata-Ishiguro M, Tsuchiya T. Effect of sulfated hyaluronan on keratinocyte differentiation and Wnt and Notch gene expression. Biomaterials 2007;28:844–850.
16. Maio AD, Vaga VL, Contreras JE. Gap junctions, homeostasis, and injury. J Cell Physiol 2002;191:269–282.
17. Tsuchiya T. Hata H, Nakamura A. Studies on the tumor-promoting activity of biomaterials: Inhibition of metabolic cooperation by polyetherurethane and silicone. J Biomed Mater Res 1995;29: 113–119.
18. Tsuchiya T, Takahara A, Cooper SL, Nakamura A. Studies on the tumor-promoting activity of polyurethanes: Depletion of inhibitory action of metabolic cooperation on the surface of a polyalkyleneurethane but not a polyetherurethane. J Biomed Mater Res 1995;29:835–841.
19. Nakaoka R. Tsuchiya T. Sakaguchi K, Nakamura A. Studies on *in vitro* evaluation for the biocompatibility of various biomaterials: Inhibitory activity of various kinds of polymer microspheres on metabolic cooperation. J Biomed Mater Res 2001;57:279–284.
20. Nakaoka R, Tsuchiya T, Nakamura A. The inhibitory mechanism of gap junctional intercellular communication induced by polyethylene and the restorative effects by surface modification with various proteins. J Biomed Mater Res 2001;57:567–574.
21. Nagahata M, Nakaoka R, Teramoto A, Abe K, Tsuchiya T. The responses of normal human osteoblasts to anionic polysaccharide polyelectrolyte complexes. Biomaterials 2005;26:5138–5144.
22. Nakaoka R, Tsuchiya T. Enhancement of differentiation and homeostasis of human osteoblasts by interaction with hydroxyapatite in microsphere form. Key Eng Mater 2006;09–311:1293–1296.
23. Tanahashi M, Matsuda T. Surface functional group dependence on apatite formation on self-assembled monolayers in a simulated body fluid. J Biomed Mater Res 1997;34:305–315.
24. Hamano T, Chiba D, Nakatsuka K, Nagahata M, Teramoto A, Kondo Y, Hachimori A, Abe K. Evaluation of a polyelectrolyte complex (PEC) composed of chitin derivatives and chitosan, which promotes the rat calvarial osteoblast differentiation. Polym Adv Technol 2002;13:46–53.
25. Ohyama M, Suzuki N, Yamaguchi Y, Maeno M, Otsuka K, Ito K. Effect of enamel matrix derivative on the differentiation of C2C12 cells. J Periodontol 2002;73:543–550.
26. Wade MH, Trosko JE, Schlindler M. A fluorescence photobleaching assay of gap junctional-mediated communication between human cells. Science 1986;232:525–528.
27. Ito Y. Surface micropatterning to regulate cell functions. Biomaterials 1999;20:2333–2342.
28. Hamilton DW, Brunette DM. The effect of substratum topography on osteoblast adhesion mediated signal transduction and phosphorylation. Biomaterials 2007;28:1806–1819.
29. Bertilsson L, Liedberg B. Infrared study of thiol monolayer assemblies on gold: Preparation, characterization, and functionalization of mixed monolayers. Langmuir 1993;9:141–149.
30. Mrksich M, Chen CS, Xia Y, Dike LE, Ingber DE, Whitesides GM. Controlling cell attachment on contoured surfaces with self-assembled monolayers of alkanethiolates on gold. Proc Natl Acad Sci 1996;93:10775–10778.
31. McClary KB, Ugarova T, Grainger DW. Modulating fibroblast adhesion, spreading, and proliferation using self-assembled monolayer films of alkylthiolates on gold. J Biomed Mater Res 2000;50: 428–439.
32. Scotchford CA, Gilmore CP, Cooper E, Leggett GJ, Downes S. Protein adsorption and human osteoblasts-like cell attachment and growth on alkylthiol on gold self-assembled monolayers. J Biomed Mater Res 2002;59:84–99.
33. Cox JD, Curry MS, Skirboll SK, Gourley PL, Sasaki DY. Surface passivation of a microfluidic device to glial cell adhesion: A comparison of hydrophobic and hydrophilic SAM coatings. Biomaterials 2002;22:929–935.
34. Howlett CR, Evans MDM, Walsh WR, Johnson G, Steele JG. Mechanism of initial attachment of cells derived from human bone to commonly used prosthetic materials during cell culture. Biomaterials 1994;15:213–222.
35. Kilpadi KL, Chang PL, Bellis SL. Hydroxyapatite binds more serum proteins, purified integrins, and osteoblast precursor cells than titanium or steel. J Biomed Mater Res 2001;57:258–267.
36. Kidoaki S, Matsuda T. Mechanistic aspects of protein/material interactions probed by atomic force microscopy. Colloids Surf B 2002;23:153–163.
37. Lecanda F, Towler DA, Ziambaras K, Cheng SL, Koval M, Steinberg TH, Civitelli R. Gap junctional communication modulates gene expression in osteoblastic cells. Mol Biol Cell 1998;9: 2249–2258.
38. Donahue HJ, Li Z, Zhou Z, Yellowley CE. Differentiation of human fetal osteoblastic cells and gap junctional intercellular communication. Am J Physiol Cell Physiol 2000;278:C315–C322.

臨床バイオメカニクス, Vol. 30, 2009.

人工関節の不具合要因分析　第二報　人工股関節

迫田　秀行[※1]　鄭　徳泳[※1]　脇谷　滋之[※2]　天正　恵治[※3]
佐藤　道夫[※1]　土屋　利江[※1]

Factors affecting joint prosthesis failure based on analysis of retrieved components. Part 2 : Artificial hip joints.

Hideyuki SAKODA, PhD., Dukyoung JUNG, PhD., Shigeyuki WAKITANI, MD., Keiji TENSHO, MD., Michio SATO, PhD., Toshie TSUCHIYA, PhD.

Abstract

Although joint arthroplasty contributes to recovering the quality of life in patients with osteoarthritis or rheumatoid arthritis, considerable numbers of revision surgeries are performed due to failure of the joint prosthesis. It is necessary to understand factors affecting joint prosthesis failure in order to reduce the number of failures. Failed and retrieved implants provide very valuable information for identification of factors related to failure since non of the tests, including in vitro mechanical tests, animal tests and clinical trials, can fully simulate the complex biological and biomechanical environment over the long term in vivo.

However, most retrieved implants are old and were manufactured by outdated technologies. Therefore, for efficient analysis of retrieved implants, it would be desirable that failures due to well known factors that have already been addressed are screened out of these analyses, preferably without collecting clinical information, since the collection and analysis of these data are costly and time-consuming.

In this study, 16 retrieved hip implants were obtained without clinical information and visually inspected followed by FTIR analysis of UHMWPE components.

Oxidative degradation of the UHMWPE components, which is known as a major factor contributing to implant failure, was considered the reason for failure in most cases. These cases could be eliminated by visual inspection. The remaining three cases were considered to have failed due to factors other than oxidative degradation of UHMWPE components. Identification of factors related to failure of these cases by detailed analysis using clinical information is expected to provide useful information for the development of future implants.

Key words : joint prosthesis, retrieved implants, UHMWPE, implant failure, oxidation.

臨床バイオメカニクス，Vol. 30，2009.

※ 1　国立医薬品食品衛生研究所　療品部
〒158-8501　東京都世田谷区上用賀1-18-1
※ 2　大阪市立大学　整形外科
〒545-8585　大阪市阿倍野区旭町1-4-3
※ 3　信州大学　整形外科
〒390-8621　長野県松本市旭3-1-1

Corresponding Author : Hideyuki Sakoda, PhD.
National institute of health sciences, Division of Medical Devices
Kamiyoga 1-18-1, Setagaya-ku, Tokyo 158-8501, JAPAN
Tel : 03-3700-9264　　Fax : 03-3700-1487
E-mail address : sakoda@nihs.go.jp

緒　　言

人工関節置換術は変形性関節症や関節リウマチの患者のQOLの改善に非常に有効な治療法であり，国内における適用数も毎年増加している[8]．しかし，不具合により再置換を余儀なくされる事例も少なくないため，その長寿命化や不具合の低減が求められている．

例えば，人工股関節においては，摺動面に使用される超高分子量ポリエチレン（UHMWPE）コンポーネントの摩耗とそれに対する生体反応が主な不具合の要因とされ，UHMWPEの酸化劣化を促進し摩耗量の増大につながる空気中におけるガンマ線照射滅菌の廃止や，摩耗特性が著しく向上した高密度架橋UHMWPEの導入などが行われた[5]．このような改良の効果は臨床導入前に様々な方法により評価されるが，関節シミュレータや疲労試験などの工学的試験では，複雑な生体内環境の再現は不可能で，また，動物実験や臨床試験では長期の試験が不可能である．従って，最終的な判断には長期の臨床成績が欠かせないが，現在得られているのは短期の臨床成績のみである[4]．

このような改良は日々なされていると考えられるが，一つの改良により別の問題が顕在化することや，新たな問題を引き起こすことも考えられ，より早期に不具合の要因を特定し，対策を施すことが必要である．そのために，現在入手可能な不具合抜去インプラントから，既知の対策の施された要因による不具合をスクリーニングにより除き，有用な情報を得ることが考えられる．

人工関節の不具合要因解析には臨床情報の分析が必須であるが，常に必要とされる情報が全て得られるわけではなく，得られたとしても分析に必要な時間やコストも膨大になる．我々は人工膝関節を対象にした研究で，臨床情報がなくても効率的にスクリーニングが可能であることを報告した[6]．本研究では，不具合で抜去された人工股関節を対象とし，効率的な抜去インプラント解析による不具合要因の推定方法について検討した．

材料および方法

1994年から2005年までの間に，信州大学整形外科において再置換術のため抜去され，入手可能であった人工股関節16例のうち，UHMWPEコンポーネントを含む15例を対象とした．初めに，各コンポーネントを観察し，破損や傷の状況を記録した．次に，フーリエ変換赤外分光光度計（FTIR）によりUHMWPEコンポーネントの分析を行った．リム部および摺動部よりリム端面あるいは摺動面に垂直に厚さ約200 μmの薄片を作製し，透過法により測定を行った．ガンマ線照射の有無を判定するため，965cm^{-1}

のトランスビニレンに起因するピークを1,370cm^{-1}付近のUHMWPEに起因するピークで正規化し，トランスビニレン指数[2]（TVI）を算出した．酸化の程度は1,720cm^{-1}付近のピークを1,370cm^{-1}付近のピークで正規化することで得られる，酸化度[1]（OI）により評価した．測定はリム端面から周方向あるいは摺動面から深さ方向に繰り返して行った．材料中でほぼ均一と考えられるTVIは測定値の平均を用い，OIについては測定値の最大値を用いた．種々の線量で照射した試験片のTVIを求め，これを検量線として，各試験試料の照射線量を推定した．Controlとして，シート成型された未滅菌のUHMWPE（GUR 1020）を使用した．

結　果

表１に目視観察およびFTIR測定の結果を示す．なお，FTIR測定は可能な限りリムから周方向と摺動面から深さ方向の少なくとも２点で行っているが，ここではこれらを合わせた結果を示す．また，最大OIの大きい順に整理している．

全ての試料で，滅菌で使用されると思われる25kGyを超える照射があったものと推定された．最大OIは，2.3から21.9まで広範に分布していた．15例中７例でリム付近におけるデラミネーションが観察された（図１）．また，４例では摺動面の荒れが観察された（図２）．15例

表１．Results of visual inspection and FTIR analysis.

Sample ID	Average TVI	EST. IRD. [kGy]	Max OI	Crystallinity [%]	Visual Inspection		
#8	0.026	70	21.9	73		rough wear surface	Yellow stain
#14	0.025	67	19.4	76	Delamination		Yellow stain
#13	0.021	57	18.6	73	Delamination		Yellow stain
#2	0.025	67	16.4	75	Delamination		Yellow stain
#6	0.028	74	12.4	75			Yellow stain
#10	0.020	54	10.9	72		rough wear surface	Yellow stain
#11	0.024	65	10.8	71			Yellow stain
#7	0.029	77	7.9	78	Delamination		Yellow stain
#5	0.026	69	7.2	74	Delamination		Yellow stain
#1	0.014	38	6.6	69	Delamination	rough wear surface	Yellow stain
#4	0.021	56	6.2	73	Delamination		Yellow stain
#9	0.015	41	4.6	67		rough wear surface	Yellow stain
#15	0.012	32	3.8	67			
#3	0.022	58	2.8	81			
#12	0.011	28	2.3	64			

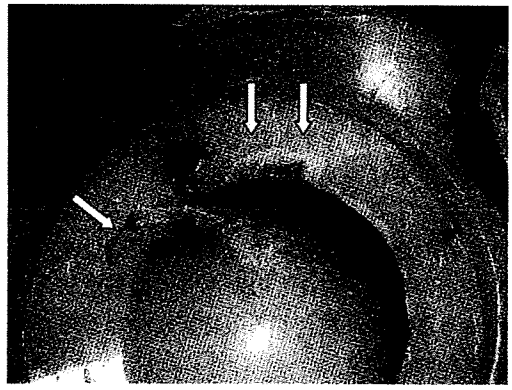

図１．Delamination at the rim of UHMWPE acetabular component（#1).

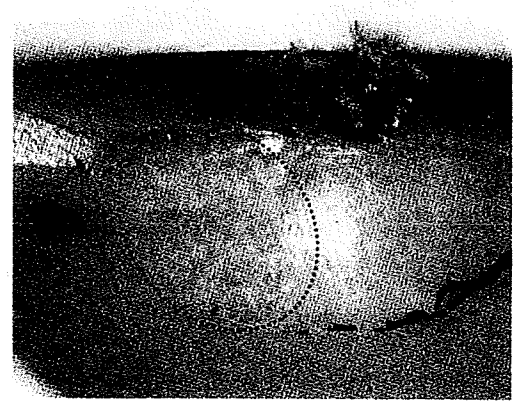

図２．Roughening of the articular surface of UHMWPE acetabular component（#1).

中12例で脂質の取り込みによると思われるコンポーネントの黄色化が見られた．しかし，脂質によると思われる1,740cm^{-1}のピーク[3]は，UHMWPEの酸化によるピークに比べ小さく（図示していない），OIの算出への影響は小さいものと思われた．人工膝関節の分析では，最大OIが4以上の場合にデラミネーションなど酸化劣化に起因すると思われる損傷が見られたが[6]，本研究でもデラミネーションや摺動面の荒れは最大OIが4以上の場合にのみ観察された．

金属製コンポーネントでは，抜去に伴うものと思われる傷が散見されたが，直接不具合の要因と推定できる破損，変形，摩耗などは見られなかった．摺動面では，バイポーラ型人工股関節のアウターヘッドを含め，摩耗を促進すると思われる顕著な傷などは見られなかった．ステムは2例（#13，#15）がセメントレスタイプであったが，どちらもメッシュ部分に骨組織がよく進入しており，良好な固定性が示唆された（図3）．残る13例はセメントタイプであったが，表面仕上げは全てがつや消し仕上げで，鏡面仕上げのものはなかった．ステム先端で光沢を持った部分が見られるものが2例（#4，#10）あり（図4），生体内におけるステムの動揺を示唆しているものと思われた．

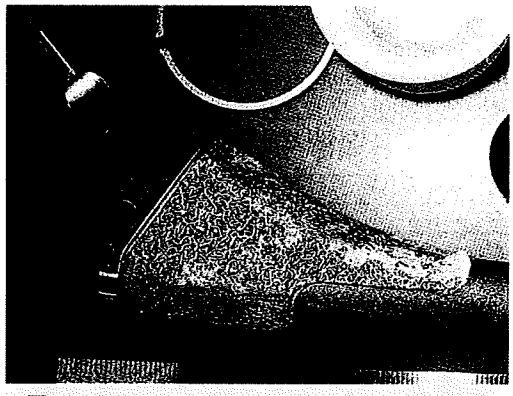

図3．Bone infiltration on meshed surface of cementless stem（#15）.

図4．Scratches at the distal end of the stem（#4）.

考　　察

人工股関節では，ある程度のインピンジの発生は避けられない．今回の試料では，ほぼ半数でリム部のデラミネーションが観察されたが，これらの試料は全て最大OIが4以上の試料であった．このことから，酸化劣化による疲労特性の低下と，インピンジによる繰り返し力の複合作用により，リム部におけるデラミネーションが発生したものと考えられた．現在市販されている製品では今回見られたような激しい酸化劣化を生じるものはないと思われるが，何らかの理由で疲労特性の低いものがあった場合，リム部におけるデラミネーションの可能性があると思われた．ただし，今回使用した試料は比較的古く，抜去してからの経過年数も長いため，保管期間中に酸化が進行していることも考えられる．その場合には，酸化の程度がより小さい時点でデラミネーションが発生していたことになり，今後も詳細に検討する必要があると思われる．

一方，摺動面の荒れは，通常の摺動面で生じる凝着摩耗以外の摩耗機構が生じていた可能性を示唆している．この事象も酸化劣化した試料でのみ生じており，今後検討する必要があると思われる．

金属製コンポーネントの観察からは不具合につながる情報があまり得られなかった．本研究の対象となったステムでは，表面仕上げが全てつや消し仕上げであった．ステムの表面仕上げについては，つや消し仕上げに対する鏡面仕上げの優位性に関する報告があるが[7),9)]，本研究の結果が不具合の発生率の違いによるものかどうかはわからなかった．ステムの動揺性を示唆する傷が観察されたものがあり，臨床情報とあわせることで不具合要因の特定につながるものと思われた．

15例中12例で，UHMWPEの酸化劣化とそれに伴うUHMWPEコンポーネントの損傷が見ら

れた．これ以外の３例では，インプラントからは不具合の要因を示唆する情報が得られず，臨床情報の解析により不具合要因の分析が必要であると考えられた．

結　　論

今回調査した15例中７例で，リム部のデラミネーションが観察された．ガンマ線照射に起因するUHMWPEの酸化劣化と，インピンジによる繰り返し力によるものと考えられた．現在市販されている製品で，同様の酸化劣化が起こることは考えにくいが，疲労特性の低下により破損が生じる可能性を示唆しており，今後も検討を要するものと考えられる．

15例中３例で，UHMWPEの酸化劣化が見られず，金属製コンポーネントにも顕著な傷などが見られなかった．これらの症例では，不具合要因の特定のためには臨床情報の解析が必要であると考えられた．人工股関節の場合も人工膝関節の場合と同様に，多くの不具合はUHMWPEの酸化劣化に起因しており，また，目視などによる判別が可能であった．目視などによりこれら以外の症例を抽出し，臨床情報を含めた詳細な解析を行うことにより，次世代型人工関節の開発や承認審査に有益な情報を効率的に収集することが可能になると考えられた．

＜謝　　辞＞

本研究は厚生労働科学研究費　医薬品医療機器等レギュラトリーサイエンス総合研究事業「医療機器・医用材料の安全性評価手法開発に関する研究」および安心安全次世代医療機器事業費による成果である．

文　　献

1）ASTM F2102-01 : Standard guide for evaluating the extent of oxidation in ultra-high-molecular-weight polyethylene fabricated forms intended for surgical implants.

2）ASTM F2381-04 : Standard test method for evaluating trans-vinylene yield in irradiated ultra-high-molecular-weight polyethylene fabricated forms intended for surgical implants by infrared spectroscopy.

3）Costa L, Bracco P et al. : Analysis of products diffused into UHMWPE prosthetic components in vivo. Biomaterials 22 : 307-315, 2001.

4）Digas G, Karrholm J et al. : Clinical performance of highly cross-linked PE with 5 year follow-up. Orthopaedic Research Society, 53rd Annual Meeting 53 : 392, 2007.

5）Kurtz SM, Muratoglu OK et al. : Advances in the processing, sterilization, and crosslinking of ultra-high molecular weight polyethylene for total joint arthroplasty. Biomaterials 20 : 1659-1688, 1999.

6）迫田秀行，鄭徳泳 他：人工関節の不具合要因分析．日本臨床バイオメカニクス学会誌 29：361-365，2008.

7）Scheerkinck T and Casteleyn PP : The design features of cemented femoral hip implants. Journal of Bone and Joint Surgery 88B : 1409-1418, 2006.

8）株式会社矢野経済研究所：2008年版メディカルバイオニクス（人工臓器）市場の中期予測と参入企業の徹底分析．19：2008.

9）Zhang HY, Blunt L et al. : Femoral stem wear in cemented total hip replacement. Proceedings of the Institution of Mechanical Engineers, Part H 222 : 583-592, 2008.

臨床バイオメカニクス, Vol. 30, 2009.

微小試験片を用いた高密度架橋ポリエチレンの疲労特性評価

迫田 秀行[※1] 石川 格[※1] 鄭 徳泳[※1] 脇谷 滋之[※2]
天正 恵治[※3] 佐藤 道夫[※1] 土屋 利江[※1]

Fatigue property of highly crosslinked polyethylene evaluated using small specimens.

Hideyuki SAKODA, PhD., Itaru ISHIKAWA, PhD., Dukyoung JUNG, PhD.,
Shigeyuki WAKITANI, MD., Keiji TENSHO, MD., Michio SATO, PhD.,
Toshie TSUCHIYA, PhD

Abstract

Highly crosslinked polyethylene (HXLPE) was introduced due to its superior wear property compared to conventional ultra-high molecular weight polyethylene (UHMWPE). The manufacturing process of HXLPE includes radiation crosslinking and thermal treatment to eliminate free radicals. Since these processes are known to degrade the fatigue property of UHMWPE, it might become one of the main factors limiting the durability of implants.

The fatigue property of UHMWPE has mainly been evaluated by fatigue crack propagation test using compact tension specimens. However, this cannot be applied to retrieved implants or final products due to the required specimen size. Therefore, there is not sufficient data to relate the fatigue property of UHMWPE to clinical outcome. The authors have developed a new test method using small specimens for evaluation of fatigue property applicable to retrieved components or final products. This study directly compares the fatigue property of HXLPE and retrieved components using the same test method.

HXLPE samples were prepared from a virgin sheet-compression-molded UHMWPE by gamma-irradiation in vacuum followed by thermal treatment above and below the melting temperature. An initial crack was created at the centre of the specimens and cyclic tensile load was applied at 1Hz by a conventional fatigue testing machine. Nominal stress and the number of cycles until fracture were used for analysis. The results were compared to those of retrieved components tested in the same manner.

HXLPE that was gamma irradiated at 100kGy followed by melt treatment showed 30% reduction in the stress level of the fatigue property. This reduction in fatigue property was similar to that of a retrieved component which showed oxidation and delamination. This result indicated the possibility of fatigue-related failure of HXLPE components depending on its manufacturing process, condition and design.

臨床バイオメカニクス，Vol. 30，2009.

Key words : joint prosthesis, crosslinked polyethylene, fatigue, retrieved implants, implant failure.

※ 1　国立医薬品食品衛生研究所　療品部
〒158-8501　東京都世田谷区上用賀1-18-1
※ 2　大阪市立大学　整形外科
〒545-8585　大阪市阿倍野区旭町1-4-3
※ 3　信州大学　整形外科
〒390-8621　長野県松本市旭3-1-1

Corresponding Author : Hideyuki Sakoda, PhD.
National institute of health sciences, Division of Medical Devices
Kamiyoga 1-18-1, Setagaya-ku, Tokyo 158-8501, JAPAN
Tel : 03-3700-9264　　Fax : 03-3700-1487
E-mail address : sakoda@nihs.go.jp

緒　　言

人工関節の寿命を制限する要因は手技上の問題も含め多岐にわたるが，中長期における主な要因は摺動面材料である超高分子量ポリエチレン（Ultra-high molecular weight polyethylene, UHMWPE）の摩耗により発生する摩耗粉に起因する人工関節のゆるみである[12]．ガンマ線照射や電子線照射によりUHMWPEに架橋を施した高密度架橋UHMWPE（Highly crosslinked UHMWPE, HXLPE）は，その優れた摩耗特性のため急速に普及した[10]．このような製品の短期臨床成績は良好であり[6]，今後人工関節の長寿命化が進むことが期待される．

しかし，HXLPEの製造に必要な，架橋を施すためのガンマ線あるいは電子線の照射や，酸化劣化を抑制するための熱処理は，いずれもUHMWPEの疲労特性を低下させることが報告されている[3),4),7),8]．人工関節には設計上多くの切り欠きや突起が存在し，その上，長期にわたり繰り返し荷重にさらされる．また，バイポーラ型人工股関節では，リム部のインピンジが不可避であるなど，疲労特性が問題になる可能性が高い．従って，摩耗による問題が解決されても，UHMWPEの疲労特性が将来的に人工関節の寿命を制限する要因になる可能性が考えられる．

HXLPEも含め，UHMWPEの疲労特性はcompact tension（CT）試験片やmiddle tension（MT）試験片を用いた疲労き裂成長試験により評価されることが多い[1]．この試験法では，繰り返し荷重下におけるき裂先端における応力状態を示す応力拡大係数幅ΔKに対する疲労き裂の成長速度da/dNを測定する．例えば，Coleらは，ガンマ線の照射量が増加するにつれ，き裂が成長を開始するΔKの下限値ΔKthが減少し，100kGyを照射した試料ではvirginの試料に比べ約30%低下すると報告した[4]．しかしこの試験法では，必要とする試験片の寸法が大きく，抜去インプラントに適用できない．実際に，不具合により抜去されたインプラントの疲労特性について報告された事例は殆どなく，疲労特性の低下と不具合の発生の関連についての知見が不足している．

我々は抜去インプラントや最終製品の試験が可能な疲労特性評価法を開発し，不具合により抜去された人工膝関節のUHMWPEコンポーネントについて疲労特性を評価した結果を報告した[11]．本研究の目的は，試作したHXLPEについて，抜去インプラントと同様の条件で試験す

ることにより，HXLPEの疲労特性について評価することである．

材料および方法

図1に試料の作製方法を示す．シート成型されたUHMWPE（GUR1020）から機械加工により4 mm×8 mm×24mmの試験片を28本作製した．この内12本はガンマ線照射も熱処理も行わないvirgin試料とした．残りの16本については，真空中にて100kGyのガンマ線照射を行い，架橋試料とした．架橋試料のうち6本は，熱処理を行わない試料（G100N）とし，ガンマ線照射後，室温，真空中で約1ヵ月保管した．残りの架橋試料のうち半量は，ガンマ線照射後，真空乾燥機（VO. 4，清水理化学機器製作所）を用い，真空中110℃で2時間アニーリング処理を行った（G100A）．また，残りの半量は同様に真空中150℃で2時間溶融処理を行った（G100R）．

各試験片の一部から回転式ミクロトーム（PR-50，大和光機工業）により，厚さおよそ200umの試料を切り出し，フーリエ変換式赤外分光光度計（FTIR，SPX200，日本電子）により測定を行った．Oxidation index[2]により，一連の処理による酸化の有無を確認した．また，以下の式に従い，結晶化度を算出した[5]．

Crystallinity[%]＝(A1896/A1305)/(A1896/A1305＋0. 25)×100

ただし，A1305とA1896はそれぞれ1,305cm^{-1}と1,896cm^{-1}におけるピーク面積である．

疲労特性評価は以前と同様に行った[11]．具体的には，試験片中央の片側にカッターで初期き裂を作製後，試験片の長軸方向の両端を汎用の疲労試験機（サーボパルサー EHF-LV010K1-A10，島津製作所）に固定し，試験片の長さ方向に最大荷重280～480N，応力比0. 1，1Hzの正弦波引張荷重を加えた．試験は100万サイクルまで行った一部の試験片を除き，10万サイクルまで行い，破断までのサイクル数で評価した．初期き裂の大きさは破断面より測定した．

破断面の観察は走査型電子顕微鏡（SEM，JSM-5800LV，日本電子株式会社）により行った．

結　果

破断面の光学顕微鏡写真から推定された初期き裂長さは0. 64mm～2. 46mmであった．

FTIR測定の結果を図2に示す．G100NとG100Aでわずかな酸化度の上昇が見られたが，その程度は小さく，一連の架橋処理による材料の酸化は無視できる程度であった．G100NとG100Aでは，結晶化度の上昇が見られたが，G100Rでは結晶化度の低下が見られた．

疲労試験の結果を図3に示す．なお，本図で

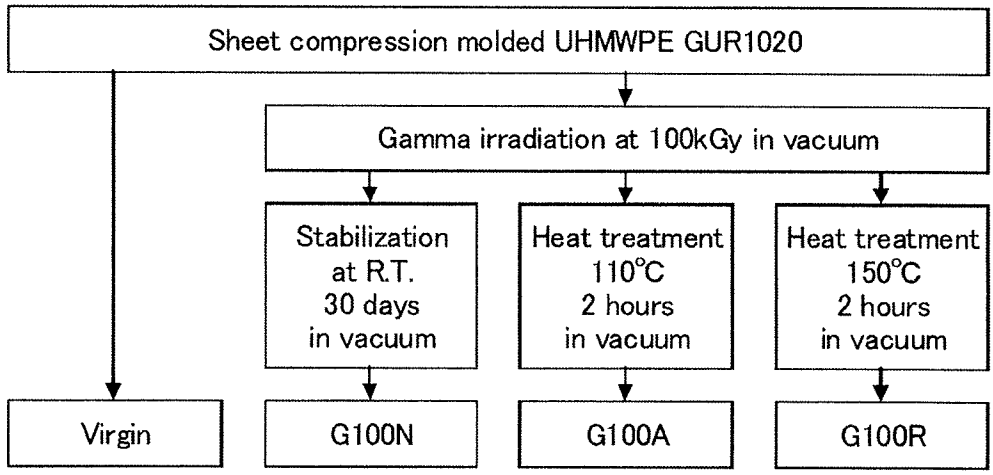

図1．Manufacturing process of specimens used in this study.